*Coordination Chemistry Reviews*, 105 (1990) 251–268
Elsevier Science Publishers B.V., Amsterdam



# KINETICS AND MECHANISM OF THE Mn(III)GLUCONATE CATALYZED DECOMPOSITION OF HYDROGEN PEROXIDE

M. E. REREK*, I. WEIL, AND M. HILL

Unilever Research United States, Inc., 45 River Road, Edgewater, New Jersey 07020 (U.S.A.)

## SUMMARY

The reaction of Mn(III) with hydrogen peroxide, in the presence of sodium gluconate, was studied at pH 10. Hydrogen peroxide was held constant at 20.0 mM, Mn(III) was varied from 0.0102-0.364 mM, and gluconate varied from 1.82-18.2 mM. Under these conditions, hydrogen peroxide was catalytically decomposed. The reaction was shown to be second-order in total [Mn(III)] and minus first-order in gluconate. The overall rate was calculated as 250 $M^{-1}sec^{-1}$. Several mechanisms were evaluated. A mechanism in which the reaction of a manganese-gluconate dimer with hydrogen peroxide was rate determining was selected on the basis of the best agreement with experimental results. Speculation on the catalytic process was proposed.

## INTRODUCTION

The use of hydrogen peroxide as a bleach for home laundering has its origins at the beginning of this century. In 1898 Tanatar (ref. 1) discovered a variety of solids which contain hydrogen peroxide. These solids fall into two general classes; hydrates of hydrogen peroxide such as sodium carbonate sesqui(peroxyhydrate), $2Na_2CO_3 \cdot 3H_2O_2$ (also known as sodium percarbonate), and true peroxides such as sodium peroxyborate tetrahydrate, $NaBO_3 \cdot 4H_2O$ (also referred to as sodium perborate tetrahydrate). Both types of solids provide convenient sources of hydrogen peroxide when added to water. The hydrates of hydrogen peroxide release hydrogen peroxide immediately upon dissolution whereas true peroxides must undergo a hydrolysis reaction. This can be envisioned by the structure of the peroxyborate anion, elucidated by Hansson (ref. 2) in 1961 (Fig. 1).

In 1907 Henkel launched a product called Persil, an abbreviation of its two main ingredients, sodium peroxyborate tetrahydrate and sodium silicate. The use of sodium peroxyborate tetrahydrate provided a safe and stable source of hydrogen peroxide in a solid washing powder. By the 1920's all the major soap manufacturers were selling formulations containing sodium peroxyborate tetrahydrate. They were among the first to take advantage of the lower priced, larger quantities of hydrogen peroxide that became available at that time due to new electrolytic methods of synthesis. Under high temperature wash conditions, hydrogen peroxide is unmatched in both performance

0010-8545/90/$06.30 

and fabric and color safety. Today, hydrogen peroxide, in both liquid and solid forms, is still the backbone of color safe fabric bleaching around the world.

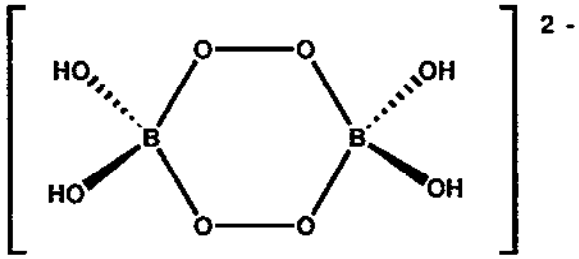


Fig. 1. Structure of the peroxyborate anion (ref. 2).

Early on, wasteful decomposition of hydrogen peroxide due to trace transition metals in the wash water was recognized. Sequestrants such as EDTA were found to minimize or prevent these interactions. Today, we are interested in preventing these decomposition reactions as well as understanding the mechanisms by which they occur.

Two general types of mechanisms, radical (outer sphere) and peroxide complex (inner sphere), have been postulated for transition metal catalyzed decompositions of hydrogen peroxide. Both mechanisms have been proposed for the Fe(III)-$H_2O_2$ system in acidic aqueous solution. The radical mechanism was proposed by Haber and Weiss (ref. 3) and elucidated by Barb, Baxendale, George, and Hargrave (ref. 4). This mechanism is shown in Scheme I. The key features of this mechanism are the discrete formation of hydroxyl and hydroperoxy radicals which can form a redox cycle with the Fe(II) / Fe(III) couple. Support for this mechanism was found by Walling and Goosen (ref. 5), who determined the inhibiting effect of organic substrates on the decomposition reaction and concluded that it was kinetically consistent with the radical scheme.

Scheme I

$$Fe(III) + H_2O_2 \longrightarrow Fe(II) + H^+ + HO_2\cdot \quad (1)$$
$$Fe(II) + H_2O_2 \longrightarrow Fe(III) + OH^- + HO\cdot \quad (2)$$
$$HO\cdot + H_2O_2 \longrightarrow H_2O + HO_2\cdot \quad (3)$$
$$Fe(III) + HO_2\cdot \longrightarrow Fe(II) + H^+ + O_2 \quad (4)$$
$$Fe(II) + HO_2\cdot \longrightarrow Fe(III) + HO_2^- \quad (5)$$

The peroxide complex mechanism was proposed by Kremer and Stein (ref 6). The significant difference in the peroxide complex mechanism (Scheme 2) is the two

electron oxidation of Fe(III) to Fe(V) with the resulting breaking of the peroxide oxygen-oxygen bond. This mechanism is favored for iron heme biological systems such as Cytochrome P-450 where formation of highly energetic free radicals is unfavored. Some mechanistic support for this mechanism was found by Groves and Van Der Puy (ref. 7) in the stereochemistry of the hydroxylation products of cyclohexanol and 7-norbornanol with Fe(III)-$H_2O_2$ . It should be noted that the solvent system used in this study was acetonitrile with water (from the $H_2O_2$ solution).

Scheme II

$$Fe(III) + H_2O_2 \rightleftharpoons Fe(III)(OOH) + H^+ \quad (6)$$

$$Fe(III)(OOH) + H_2O_2 \longrightarrow Fe(V)O + OH^- \quad (7)$$

$$Fe(V)O + H_2O_2 \longrightarrow \longrightarrow Fe(II) + H_2O + O_2 \quad (8)$$

Both mechanisms could represent the two extremes of the same process. Free radicals may only be generated within the solvent cage of the complex and react therein; conversely, metal-peroxo complexes can be precursors for the generation of free radicals. Often it is very difficult to distinguish between these two types of mechanisms on kinetic grounds. Most studies of metal catalyzed decomposition of hydrogen peroxide do invoke free radical mechanisms to explain the kinetic findings.

In the course of our investigations, it was found that manganese in the +3 oxidation state was very effective at catalyzing the decomposition of hydrogen peroxide in alkaline solution. Kinetic studies of Mn(III) catalyzed hydrogen peroxide decomposition, in acidic or alkaline solution, are rare. The reaction of $[Mn(III)(H_2O)_6]^{3+}$ and $[Mn(III)(H_2O)_5OH]^{2+}$ with $H_2O_2$ was studied by two groups using stopped flow techniques with somewhat contradictory results. Wells and Mays (ref. 8) found the rate of reaction to be first order in Mn(III) and independent of Mn(II) and hydrogen peroxide. Davies, Kirschenbaum and Kustin (ref. 9) found the rate of reaction to be first order in Mn(III), hydrogen peroxide, and inversely dependent on Mn(II). The apparent second-order rate constant was found to decrease with increasing initial peroxide concentration. This result was attributed to the competition of Mn(III) and hydrogen peroxide for the $H_2O_2^+$ radical. It was later noted (ref. 10) that the use of the bimolecular rate equation in this study was inappropriate; a recalculation using a first order plot gave much better results which were in general agreement with those of Wells and Mays.

Complexes of Mn(III) react more slowly with hydrogen peroxide than do the Mn(III) aquo ions. Jones and Hamm (ref. 11) examined the reaction of $[Mn(III)(CyDTA)(H_2O)]^-$ (CyDTA=1,2 diaminocylohexanetetraacetate) with hydrogen peroxide and found it to be first-order in peroxide, second-order in $[Mn(III)(CyDTA)(H_2O)]^-$, and inversely dependent on both $[H^+]$ (between pH 2-4) and $[Mn(II)CyDTA)]^{2-}$ . The authors interpreted these results as consistent with a

mechanism in which a $[Mn(III)(CyDTA)(O_2H)]^{2-}$ intermediate forms and slowly decomposes to $[Mn(II)CyDTA)]^{2-}$ and $\cdot HO_2$ ; the resulting hydroperoxy radical reacts with a second $[Mn(III)(CyDTA)(H_2O)]^-$ in the rate determining step to give the second-order dependence on Mn(III).

Rizkalla, Anis, and Khalil (ref. 12) studied the reaction of $[Mn(III)(ENTMP)(OH)]^{6-}$ (ENTMP= ethylenediaminetetra(methylenephosphonic) acid) with hydrogen peroxide and observed a first-order dependence on both Mn(III) complex and hydrogen peroxide concentration. The reaction was studied under alkaline conditions of pH 9.0-10.3. The rate determining step in the proposed mechanism was formation of a $[Mn(ENTMP)(OOH)]^{6-}$ species. This complex can decompose to hydroxyl radical and a $[Mn(IV)(ENTMP)(O)]^{6-}$ species. Hydroxyl radical reacts with hydrogen peroxide to give water, proton, and superoxide radical which can then reduce the Mn(IV)-oxo complex. Under strongly alkaline conditions (above pH 11) colloidal $MnO_2$ was formed.

Sawyer and co-workers have shown (ref. 13-14) that polyhydroxy ligands can form stable complexes of Mn(II), Mn(III) and Mn(IV) in strongly alkaline solution. They focused much of their attention on sodium gluconate, the salt of the carboxylic acid fermentation product of D-glucose. Magnetic susceptibility, ESR, and electrochemical techniques were used to determine manganese oxidation state; electrochemical and spectrophotometric techniques gave insight into the nature of the complexes formed. Under the conditions studied, both monomeric and dimeric manganese-gluconate species were observed. Formation of dimeric complexes was favored at higher concentrations of manganese and lower ratios of gluconate to manganese. For Mn(III), they attributed the principal monomeric species to $[MnG_3]^{3-}$ and the principal dimeric species as $[Mn_2G_4(\mu\text{–}OH)_2]^{4-}$, where G is the bidentate gluconate ligand.

Under strongly alkaline conditions (0.3 M NaOH), oxygen rapidly converts Mn(II) and Mn(III) gluconate species to Mn(IV)gluconate species. This can be observed visually; Mn(II)gluconate species are colorless, Mn(III)gluconate species are yellow to brown, and Mn(IV) gluconate species are crimson red. These oxidations are reversable upon the addition of acid to the solutions. Bodini and Sawyer (ref. 14) examined the kinetics of the oxidations of manganese-gluconate species with oxygen and hydrogen peroxide. The reaction of Mn(II)gluconate and oxygen is first-order in both reactants. This reaction is very fast, the rate constant being $2.8 \times 10^4\ M^{-1}sec^{-1}$. When hydrogen peroxide is used, the reaction is much slower; the rate constant is 0.6 $M^{-1}sec^{-1}$. The stoichiometry of the reaction with hydrogen peroxide was dependent on the gluconate concentration. Oxidation of Mn(III)gluconate to Mn(IV)gluconate by oxygen was only achieved at lower gluconate concentrations. This strongly implies that only the dimeric Mn(III)gluconate species is reactive. Hydrogen peroxide does not react with monomeric or dimeric Mn(III)gluconate species to afford Mn(IV)gluconate under these conditions.

Sawyer's findings are significant for manganese in alkaline solution; Mn(III) is unstable with respect to diproportionation, and manganese dioxide is very thermodynamically favored. Ligands which stabilize Mn(II) and Mn(III) often do not form strong complexes with Mn(IV). This was true for the manganese-ENTMP system discussed above. Ligands which form strong complexes with the three major oxidation states of manganese in aqueous solution insure that the decomposition reaction with hydrogen peroxide will remain homogeneous.

One kinetic study of Mn(III) complexed by polyhydroxy ligands has been reported in the literature. Guindy, Daoud, and Milad (ref. 15) found that the reaction of Mn(III)citrate with hydrogen peroxide was first-order in both Mn(III) and hydrogen peroxide at neutral pH. The reaction was inversely dependent on both citrate and Mn(II) concentration. They attributed the reactive species to the uncomplexed $[Mn(H_2O)_5OH]^{2+}$. If this is the reactive species, it is much less reactive at pH 7 than under the strongly acidic conditions studied by Wells (ref. 8) and Davies (ref. 9).

We have examined the decomposition of hydrogen peroxide catalyzed by Mn(III)gluconate at pH 10 as a function of gluconate and manganese concentrations. The results of these experiments and proposed mechanisms are discussed below.

## EXPERIMENTAL

Solid Mn(III)gluconate can be prepared in a matrix of sodium gluconate. It was typically prepared by dissolving sodium gluconate and manganese(II)sulfate in a 10:1 mole ratio in doubly deionized water. The pH of the solution was adjusted to 10 with 1 M NaOH and oxidation accomplished by vigorous stirring in air. Oxidation was usually complete after 1 hour (25-100g scale). Water was then removed through rotatory evaporation or freeze drying. The solid was then collected and homogenized by grinding to a fine powder. Manganese content in the solids was determined by atomic absorption spectroscopy; these numbers were used to prepare solutions. Oxidation state was determined using the Evan's method (ref. 16). Stable, dry solids containing Mn(III) could be obtained from 5/1 to 100/1 gluconate/manganese ratios using this technique.

Hydrogen peroxide decomposition reactions were studied at 40°C in double deionzed water using a 2 l jacketed glass beaker. Psuedo-first-order conditions were maintained with an initial concentration of 0.02 M hydrogen peroxide, and Mn(III) varied from 0.0103 mM - 0.364 mM. Solutions of 30% hydrogen peroxide and the 10:1 gluconate to manganese solid were the sources of these materials. Excess sodium gluconate was added as the solid where appropriate. Carbonate buffer was used to maintain the pH of the solution at 10.0. Reaction rates were measured by the loss of hydrogen peroxide as a function of time. Removal of 5 ml aliquots at appropriate intervals into flasks containing 10 ml of 4 N $H_2SO_4$ efficiently quenched the reaction. These were subsequently analyzed using iodometric titration for residual peroxide using a Brinkmann Metrohm 672 autotitrator. Reaction rates were calculated from the

slope of psuedo-first-order plots of ln [$H_2O_2$ ] vs. time. All rates were the average of at least two experiments; most were of three runs.

## RESULTS

Under the conditions studied, these reactions afford linear plots of ln [$H_2O_2$] vs. time for greater than three half lives. Several examples are shown in Fig. 2. The linearity of these plots demonstrate that the assumption of psuedo-first-order behavior is valid; thus these reactions are truly catalytic in manganese. Some curvature was observed at the end of the reactions when the psuedo-first-order assumption was no longer valid.

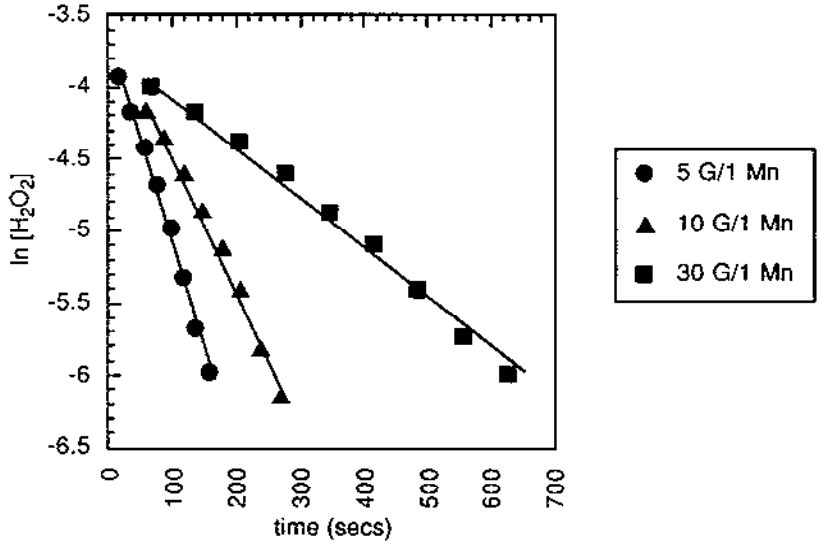


Fig. 2. First-order plot of ln [$H_2O_2$] vs. time for the Mn(III)gluconate catalyzed decomposition of hydrogen peroxide. Legend refers to the ratio of gluconate to manganese in each reaction.

Table 1 shows the rate of Mn(III)gluconate catalyzed decomposition of hydrogen peroxide as a function of gluconate concentration. As the concentration of gluconate increased, the rate of decomposition decreased. To more clearly illustrate this inhibition, the data in Table 1 is plotted in Fig. 3.

Increasing the total manganese concentration has a complex effect on the rate of decomposition. The rates of decomposition as a function of manganese concentration are given in Table 2. These experiments were conducted at a constant ratio of gluconate to manganese; as manganese concentration increases, the gluconate

concentration increases. This effect is due to the use of the solid 10 gluconate/1 manganese mole ratio material in these experiments. Under these conditions, a first order dependence on manganese concentration should produce a response which does not linearly increase with manganese due to the inhibiting effect of the increasing gluconate concentration. A somewhat linear increase was observed (Fig. 4), indicating that the reaction has a greater than first order dependence on manganese concentration.

TABLE 1

Effect of gluconate concentration of the rate of hydrogen peroxide decomposition catalyzed by Mn(III) gluocnate[a].

| [gluconate], M | $k_{obs}$ , $sec^{-1}$ | $G_T$ / $Mn_T$ | $Mn_T$ / $k_{obs}$ |
|---|---|---|---|
| 0.00182 | 0.0155 | 5 | 0.024 |
| 0.00364 | 0.00937 | 10 | 0.039 |
| 0.00728 | 0.00513 | 20 | 0.071 |
| 0.01092 | 0.00360 | 30 | 0.101 |
| 0.0182 | 0.00219 | 50 | 0.167 |

[a] [Mn] constant at 0.364 mM.

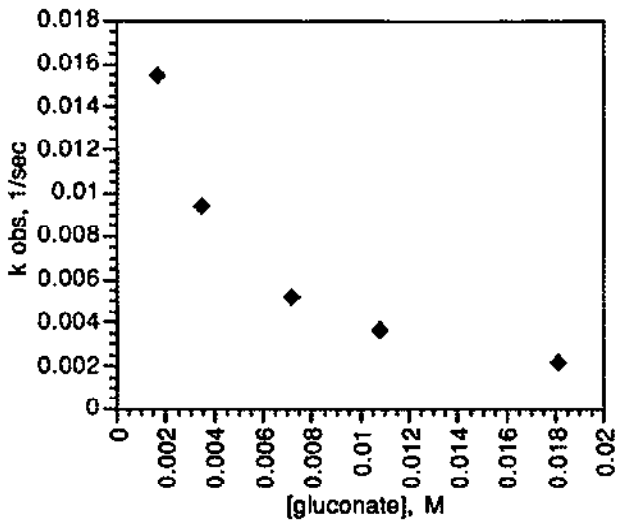


Fig. 3. Effect of gluconate concentration on the rate of Mn(III)gluconate catalyzed decomposition of hydrogen peroxide.

TABLE 2

Effect of total manganese concentration on the rate of hydrogen peroxide decomposition catalyzed by Mn(III) gluconate[b].

| [Mn], mM | $k_{obs}$ , $sec^{-1}$ | 1/ $Mn_T$ | $Mn_T$ / $k_{obs}$ |
|---|---|---|---|
| 0.0103 | 0.000134 | 2747 | 0.039 |
| 0.0182 | 0.000305 | 3663 | 0.044 |
| 0.0364 | 0.000728 | 18315 | 0.047 |
| 0.0546 | 0.001150 | 27473 | 0.050 |
| 0.273 | 0.00627 | 49261 | 0.060 |
| 0.364 | 0.00937 | 96819 | 0.077 |

[b] experiments conducted at constant mole ratio of gluconate to manganese (10).

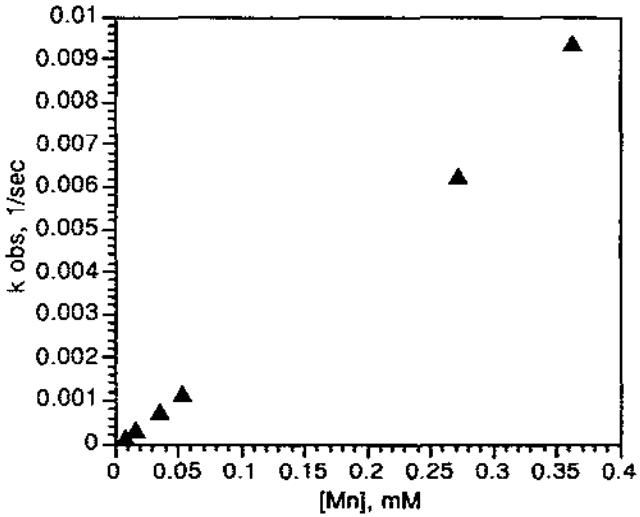


Fig. 4. Effect of total manganese concentration on the rate of the Mn(III)gluconate catalyzed decomposition of hydrogen peroxide.

## DISCUSSION

We have examined the solution chemistry of manganese with gluconate at pH 10. At this pH, oxygen oxidized Mn(II) gluconate to Mn(III)gluconate. The assignment of the +3 oxidation state to manganese under these conditions was based on the yellow brown color of the solutions as reported by Sawyer (ref. 13), and through magnetic susceptibility measurements. Typical magnetic susceptibilities were 4.58 BM, in good agreement with Sawyer. Oxygen will only further oxidize the manganese center at higher alkalinity, signaled by a color change to crimson red.

Our finding that Mn(III)gluconate reacts readily with hydrogen peroxide is in contrast to Sawyer's report that Mn(III)gluconate does not react with hydrogen peroxide. The apparent discrepancy is easily reconciled by the difference in the reaction conditions used; our work was conducted at pH 10 whereas Sawyer's was conducted at approximately 13.5. The redox potentials of both hydrogen peroxide and manganese are very sensitive to pH. Hydrogen peroxide becomes a weaker oxidant as pH increases; somewhere between 10 and 13.5 its potential becomes smaller than the Mn(III)/Mn(IV) potential.

To summarize our kinetic observations, the reaction is psuedo-first-order in hydrogen peroxide. At constant manganese concentration, there is an inverse rate relationship with respect to gluconate. Finally, at constant gluconate to manganese mole ratio, the rate increase with respect to total manganese concentration is greater than first-order.

Further kinetic analysis of this system is very difficult since the only known parameters are the observed rate constants as a function of total gluconate and total manganese concentrations. We were not able to quantitate the manganese-gluconate speciation under these conditions. Therefore, the validity of a given mechanism can only be tested if it can be reduced to a dependency on total gluconate and manganese concentration and the observed rate constants. Lack of quantitative speciation behavior between gluconate and manganese is a large hindrance to the kinetic analysis of this system.

In order to postulate a mechanism to fit these kinetic results, several assumptions must be made. The first assumption is that all manganese in the system is complexed by gluconate. This assumption is supported by Sawyer's observation of solution homogeneity under alkaline and oxidizing conditions; if gluconate wasn't strongly binding the manganese, precipitates of manganese(III)hydroxide and manganese dioxide would readily form. We have also observed this behavior under our conditions; solutions of Mn(III)gluconate remain homogeneous for weeks under storage at room temperature. A second assumption is that the major species in solution is a bis gluconatoMn(III) complex. Thirdly, we assume that this major species can dimerize with loss of a gluconate ligand (eq. 9). Finally, we assume that the manganese gluconate species is indeed the catalytic species in the decomposition (eq. 10).

A proposed mechanism is outlined in the reactions below:

Mechanism I

$$2\,[MnG_2(OH)_2]^{3-} + H_2O \underset{}{\overset{K_1}{\rightleftharpoons}} [Mn_2G_3(OH)_2(H_2O)_2]^{4-} + HG^- + OH^- \quad (9)$$

$$[Mn_2G_3(OH)_2(H_2O)_2]^{4-} + H_2O_2 \xrightarrow{k_{rds}} [Mn_2G_3(OOH)(OH)(H_2O)_2]^{4-} + H_2O \quad (10)$$

where G represents the gluconate ligand.

This is the simplest mechanism which can be written to account for the observed dependencies on hydrogen peroxide, gluconate, and total manganese concentrations. Our assumption of the major species as $[MnG_2(OH)_2]^{3-}$ is primarily for convenience. It allows for both the gluconate inhibition and the higher order dependence in manganese, shown in eq. 10. We also assume a bridging gluconate ligand which has a net 4- charge. This is discussed below. None of these assumptions impact the evaluation of Mechanism I.

The expression for the equilibrium constant $K_1$ is:

$$K_1 = [Mn_2G_3(OH)_2(H_2O)_2^{4-}] [HG^-] / [MnG_2(OH)_2^{3-}]^2 \quad (11)$$

where the hydroxide dependence was ignored due to the buffering of the system.

The material balance equations for eq 9-10 are:

$$G_T = HG^- + 2[MnG_2(OH)_2]^{3-} + 3[Mn_2G_3(OH)_2(OH_2)_2]^{4-} \quad (12)$$

$$Mn_T = [MnG_2(OH)_2]^{3-} + 2[Mn_2G_3(OH)_2(OH_2)_2]^{4-} \quad (13)$$

where $G_T$ is the total gluconate concentration, $HG^-$ is the concentration of free gluconate, and $Mn_T$ is the total manganese concentration.

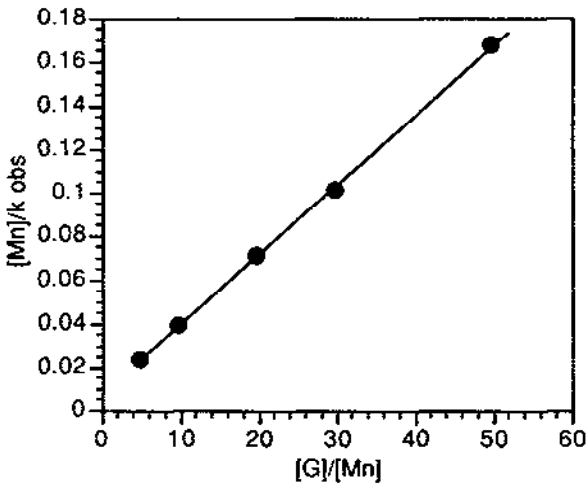


Fig. 5. Plot of $Mn_T / k_{obs}$ vs. $G_T / Mn_T$ at constant $Mn_T$. Under these conditions, linear dependence of Mn(III)gluconate catalyzed decomposition of hydrogen peroxide on gluconate concentration is observed. Both Mechanisms I and II predict this result of a linear slope with a non-zero intercept.

Solving equations 11, 12, and 13 for $[Mn_2G_3(OH)_2(OH_2)_2]^{4-}$ gives the approximate solution:

$$[Mn_2G_3(OH)_2(OH_2)_2]^{4-} = K_1 Mn_T^2 / [G_T + (4K_1 - 2)Mn_T] \quad (14)$$

where higher order terms in $[Mn_2G_3(OH)_2(OH_2)_2]^{4-}$ were assumed to be small and therefore ignored. This indeed was shown to be true when the equations were solved.

The rate equation for the loss of hydrogen peroxide in this system is given by:

$$-d[H_2O_2] / dt = k\,[catalyst]\,[H_2O_2] \quad (15)$$

$$k_{obs} = k[Mn_2G_3(OH)_2(OH_2)_2]^{4-} \quad (16)$$

where the catalyst is assumed to be $[Mn_2G_3(OH)_2(OH_2)_2]^{4-}$.

Substitution of equation 14 into equation 16 affords:

$$k_{obs} = k\,K_1 Mn_T^2 / [G_T + (4K_1 - 2)Mn_T] \quad (17)$$

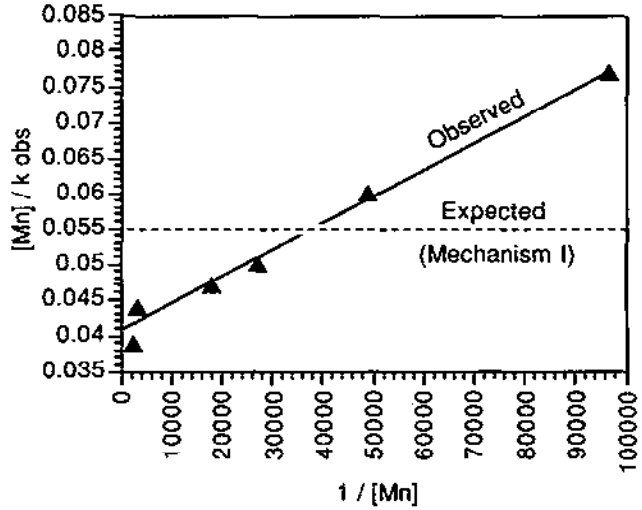


Fig. 6. Comparison of expected and observed dependence of the rate of Mn(III)gluconate catalyzed decomposition of hydrogen peroxide on $Mn_T$ at constant ratio of $G_T$ / $Mn_T$. Mechanism I predicts an invariant response. Mechanism II predicts the observed linear slope with positive, non-zero intercept.

Rearranging eq. 17 affords:

$$Mn_T / k_{obs} = (1/ k K_1)[G_T / Mn_T + 4K_1 - 2] \quad (18)$$

which allows a plotting of the experimental data to determine the relevance of the proposed mechanism.

A plot of $Mn_T / k_{obs}$ vs. $G_T / Mn_T$ at constant $Mn_T$ is shown in Fig. 5. Under these conditions, this plot gives the gluconate dependence; it essentially is a plot of $1/k_{obs}$ vs. $G_T$. The observed linear slope with a positive, non-zero intercept indicates an inverse first-order dependence on gluconate, in agreement with the prediction of the model. Under conditions where $G_T / Mn_T$ was constant, eq. 18 predicts that a plot of $Mn_T / k_{obs}$ is independent of $1/Mn_T$; however, this was not observed (Fig. 6). Instead, a positive slope was obtained. This discrepancy between the predicted and experimental results indicates that the system cannot be described by Mechanism I.

Since the general nature of the assumptions made still appear reasonable, a perturbation can be introduced to give a minor manganese dependence under the conditions of constant ratio of $G_T / Mn_T$ through two additional equilibria. These are shown in Mechanism II.

Mechanism II

$$2\,[MnG_2(OH)_2]^{3-} + H_2O \underset{}{\overset{K_1}{\rightleftharpoons}} [Mn_2G_3(OH)_2(H_2O)_2]^{4-} + HG^- + OH^- \quad (19)$$

$$[Mn_2G_3(OH)_2(H_2O)_2]^{4-} + OH^- + H_2O \overset{K_2}{\rightleftharpoons} [MnG_2(OH)_2]^{3-} + [MnG(OH)_3(H_2O)]^{2-} \quad (20)$$

$$[MnG_2(OH)_2]^{3-} + 2H_2O \overset{K_3}{\rightleftharpoons} [MnG(OH)_3(H_2O)]^{2-} + HG^- \quad (21)$$

$$[Mn_2G_3(OH)_2(H_2O)_2]^{4-} + H_2O_2 \xrightarrow{k_{rds}} [Mn_2G_3(OOH)(OH)(H_2O)_2]^{4-} + H_2O \quad (22)$$

where $K_1 = K_3 / K_2$. Using the new material balance equations:

$$G_T = HG^- + [MnG(OH)_3(H_2O)]^{2-} + 2[MnG_2(OH)_2]^{3-} + 3[Mn_2G_3(OH)_2(OH_2)_2]^{4-} \quad (23)$$

$$Mn_T = [MnG(OH)_3(H_2O)]^{2-} + [MnG_2(OH)_2]^{3-} + 2[Mn_2G_3(OH)_2(OH_2)_2]^{4-} \quad (24)$$

an approximate solution to the resulting quadratic equation (ignoring third order terms) can be obtained:

$$Mn_T / k_{obs} = (1/ k K_1 )[\ G_T / Mn_T + 4K_1 - 1 + 2K_1K_2 / Mn_T\ ] \quad (25)$$

This expression not only satisfies the inverse first-order gluconate dependence in Fig. 5, but also predicts the manganese dependence in Fig. 6. This additional manganese dependence under conditions of constant $G_T / Mn_T$ indicates that there is a true second-order dependence on $Mn_T$. Mechanism I predicts a first-order dependence on manganese at constant $G_T / Mn_T$ which was not observed.

TABLE 3

Kinetic parameters for the Mn(III)gluconate catalyzed decomposition of hydrogen peroxide calculated from Fig. 5 and 6.

| Constant | Value |
|---|---|
| $K_1$ | 0.93 |
| $K_2$ | $5.5 \times 10^{-5}$ |
| k | 340 $M^{-1}sec^{-1}$ |

Using the slopes and intercepts from the two plots allows a determination of the equilibrium constants and the true rate constant. These are shown in Table 3. On the basis of the equilibrium constants, the concentration of the assumed catalyst, $[Mn_2G_3(OH)_2(OH_2)_2]^{4-}$ , varied from 2-10% of the total manganese concentration in the kinetic experiments reported here.

Mechanism III:

$$[MnG_2(OH)_2]^{3-} + H_2O \underset{}{\overset{K_3}{\rightleftharpoons}} [MnG(OH)_3(H_2O)]^{2-} + HG^- \quad (26)$$

$$[MnG_2(OH)_2]^{3-} + H_2O_2 \overset{K_4}{\rightleftharpoons} [MnG_2(OOH)(OH)]^{3-} + H_2O \quad (27)$$

$$[MnG_2(OOH)(OH)]^{3-} + [MnG(OH)_3(H_2O)]^{2-} \xrightarrow{k_{rds}}$$

$$[Mn_2G_3(OOH)(OH)(H_2O)_2]^{4-} + OH^- + H_2O \quad (28)$$

Mechanisms I and II are obviously not the only potential mechanisms for this reaction. Another plausible mechanism involves an equilibrium between a monomeric Mn(III)gluconate species and hydrogen peroxide, followed by a rate determining reaction between the Mn(III)gluconate-hydrogen peroxide complex and another Mn(III)gluconate species. This is shown in Mechanism III. Although this mechanism has some attractive features, there are several reasons for rejection.

First, optimal estimates of the kinetic parameters for Mechanism III were obtained by a non-linear regression on the experimental data, iterating with a multivariate secant (false position) technique (ref. 17). This procedure was also used to calculate the optimal kinetic parameters for Mechanism II to augment those obtained by the approximate graph solution shown in Table 3. The resulting kinetic parameters for the two mechanisms are shown in Table 4.

For Mechanism III, individual values for the equilibrium constants could not be obtained because they were too highly correlated. Instead, the optimal ratio of the equilibrium constants $K_3$ and $K_4$ was obtained. This ratio is sufficient to calculate the rate of hydrogen peroxide decomposition.

TABLE 4
Kinetic parameters for Mechanisms II and III calculated by nonlinear regression analysis.

| Mechanism II | Mechanism III |
|---|---|
| $K_1$=1.3 | $K_3/K_4$=2.4 x $10^4$ |
| $K_2$=3.7 x $10^{-5}$ | |
| $K_3$=4.8 x $10^{-5}$ | k=5.3 x$10^6$ |
| k=250 $M^{-1}sec^{-1}$ | |

Given the results of this non-linear regression, the validity of the two mechanisms can be assessed in two ways. First, the residual sum of the squares of the differences between observed values and those calculated with optimal estimates of the kinetic parameters objectively measures the validity of a given mechanism. Thus, for each proposed mechanism, the Newton-Raphson iteration algorithm (ref. 18) was used to simultaneously solve the material balance and equilibrium equations for each experiment, using the optimal estimates of the kinetic parameters in Table 4. This provided the concentrations of all species, which could then be used to calculate the rate of decomposition (Table 5) for each experiment. These were then used to calculate the residual sum of the squares for that mechanism. The residual sum of the squares for Mechanism III (peroxy complex) indicated a greater difference with the experimental data by this method; 8.5 x $10^{-5}$ for Mechanism III vs. 4.3 x $10^{-7}$ for Mechanism II.

A second, subjective, assessment can be made by visual examination of the plot of the calculated vs. the measured rates. This is shown in Fig. 7. Perfect agreement is signaled by a 45$^o$ line. Mechanism II is very close to this line whereas Mechanism III differs to a significant extent. These results strongly indicate that the proposed peroxide complex mechanism is not as preferred as the proposed modified dimerization mechanism . For these reasons, we feel that Mechanism II best describes the kinetic process of the Mn(III)gluconate catalyzed hydrogen peroxide decomposition.

Additionally, the peroxide complex mechanism predicts a finite concentration of a Mn(III)gluconate-hydrogen peroxide complex. Under our experimental conditions, we could detect no evidence of a species of this nature. It is interesting to note that Jones and Hamm (ref. 11) could not detect $[Mn(III)(CyDTA)(O_2H)]^{2-}$ although they postulated this intermediate. In their mechanism, this species lost hydroperoxide radical which reacted with $[Mn(III)(CyDTA)(OH_2)]^{1-}$ to explain the observed second-order dependence of manganese in the peroxide decomposition reaction. They reasoned that an upper limit of 5% could be put on the hydroperoxy intermediate without greatly influencing the the visible spectrum they were measuring for kinetic analysis. The dimerization mechanism is very unfavored in this system due to the bulky, six coordinate 1,2-diaminocyclohexanetetraacetate ligand.

Further support for the dimerization mechanism comes from a report by Oishi, Nishida, and Kida (ref. 19) on the reaction of hydrogen peroxide with several Mn(III) Schiff-base complexes. The dimeric $[Mn_2(salpa)_2]Cl_2$ (salpa=N-salicylidenepropylene 2-ol) catalytically decomposes hydrogen peroxide at what they describe is a rapid rate. The mononuclear [Mn(salen)NCS] (salen=N,N'-disalicylideneethylenediamine) and [Mn(amben)NCS] (amben=N,N'-bis(o-aminobenzylidene)ethylenediamine) show little or no reaction with hydrogen peroxide under these conditions.

TABLE 5

Comparison of the measured and optimally calculated rates of decomposition for Mechanism II and Mechanism III using non-linear regression analysis.

| Measured | Mechanism II | Mechanism III |
|---|---|---|
| $k_{obs}$ , $sec^{-1} \times 10^4$ | $k_{calc}$ , $sec^{-1} \times 10^4$ | $k_{calc}$ , $sec^{-1} \times 10^4$ |
| 1.34 | 1.32 | 1.23 |
| 3.05 | 3.07 | 2.99 |
| 7.28 | 7.47 | 7.60 |
| 11.5 | 12.0 | 12.4 |
| 21.9 | 22.1 | 16.7 |
| 36.0 | 35.5 | 28.5 |
| 51.3 | 50.9 | 44.1 |
| 62.7 | 67.4 | 72.3 |
| 93.7 | 90.6 | 97.5 |
| 155 | 152 | 246 |

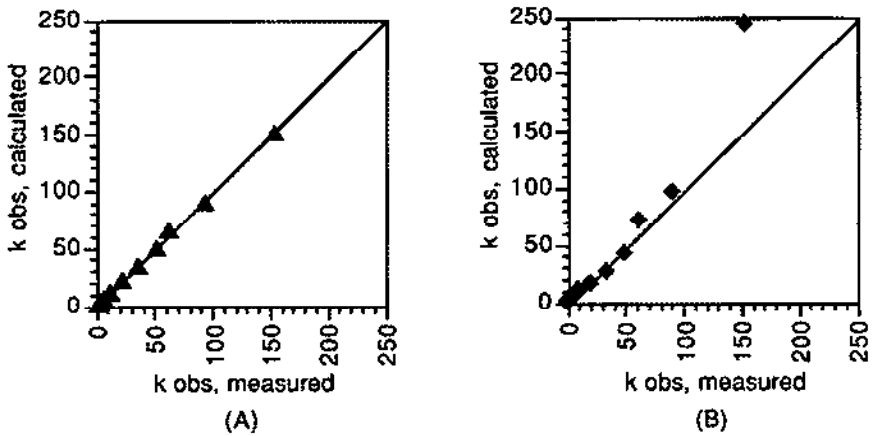


Fig. 7. Comparison of the measured vs. calculated rate values for Mechanism II (A), and Mechanism III (B). The values are all x $10^4$.

This is very similar to our proposal that only a dimeric manganese gluconate species is active in the decomposition of hydrogen peroxide. They speculate that the intermediate in the catalytic decomposition can be described by a bridging peroxo ligand between the two manganese centers. We believe that a similar intermediate is formed in the Mn(III)gluconate catalyzed decomposition of hydrogen peroxide. A catalytic scheme for this reaction is shown in Fig. 8.

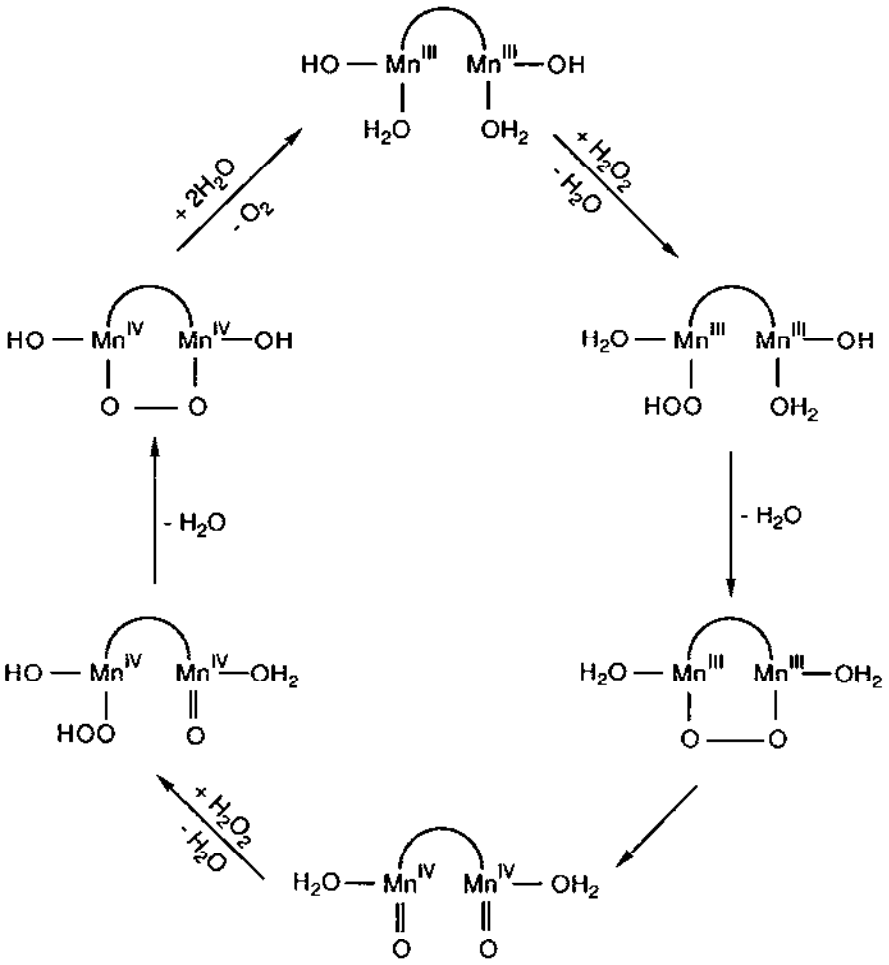


Fig. 8. Reaction scheme for the catalytic decomposition of hydrogen peroxide by Mn(III)gluconate. Nonparticipating ligands are not shown. The arc represents a bridging ligand.

After the formation of a hydroperoxy ligand in the rate determining step (eq. 22), an intramolecular nucleophilic attack can occur to form a peroxo bridged species. This is accompanied by proton uptake by a hydroxide ligand and loss of water. Oxidative cleavage of the peroxide ligand results in two Mn(IV) oxo centers. The Mn(IV)dimer can react with hydrogen peroxide such that the oxo ligand is protonated, hydroperoxide ligand is coordinated, and water is lost. A second internal nucleophilic attack occurs which protonates the second oxo ligand, forms a peroxide bridge, and a water ligand is lost. Electron transfer now occurs from the peroxide to the manganese centers which results in loss of oxygen and formation of the original Mn(III)gluconate dimer.

Variations on both the dimerization and peroxide complex mechanisms which give rise to symmetric intermediates containing the $[Mn_2G_4(OOH)]$ fragment are much less favored than the corresponding intermediates containing the $[Mn_2G_3(OOH)]$ fragment postulated in Mechanisms I-III. In general, these fail to fully satisfy the conditions of gluconate inhibition. Where this was overcome through additional equations, the resulting residual sum of the squares indicated much poorer agreement with experimental results. Although it is initially easier to conceive of the structure of symmetrical intermediates containing $[Mn_2G_4]$ fragments, these must be rejected on kinetic grounds. For these reasons, we have selected the $[Mn_2G_3]$ fragment as the principal component of the critical species in our reactions.

Although it is non-essential to our mechanism, we speculate that gluconate is the bridging ligand. Some precedence for this behavior exists in the literature. Borate ion can form a bridge between alcohol groups of two gluconates (ref. 20), and van Bekkum and co-workers (ref. 21) have shown that this species can bind aluminum in the traditional carboxylate α-hydroxy bidentate fashion. The oxophilicity of the higher oxidation states of manganese can explain the driving force for further coordination of the gluconate alcohol groups. Space filling models show that coordination of one manganese center to the carboxylate α-hydroxy head leaves ample space for coordination of a second manganese to the polyhydroxy tail. A bridging gluconate ligand allows a symmetric dimer and one whose formation would be inhibited by excess gluconate. In the end, dimers can be formed with the previously observed hydroxy bridges for Mn(III) and oxo bridges for Mn(IV) (ref. 22).

In general, we have avoided the use of radicals in our mechanisms. This is for two reasons. The first is that the apparent second-order dependence of the reaction on manganese suggests a two electron process. The formation of radicals via one electron processes which can leave a coordination sphere containing two manganese centers seems unlikely. More importantly, gluconate is a potent radical inhibitor. Rate inhibition by excess gluconate should be more effctive than rate enhancement from increasing manganese concentration for radical processes. Instead, the opposite is true; decomposition of hydrogen peroxide is quite facile in the presence of excess gluconate when appropriate concentrations of manganese were used. Although this

does not conclusively rule out radical processes, they are certainly not favored under the conditions used in these experiments.

REFERENCES


1 S.M. Tanatar, Z. Phys. Chem., 26 (1898)132-140.
2 A. Hansson, Acta. Chem. Scand., 15 (1961) 934-938.
3 F. Haber and J. Weiss, Proc. Roy. Soc. (London) A, 147 (1934) 332- .
4 W.G. Barb, J.H. Baxendale, P. George, and K.R. Hargrave, Trans. Faraday Soc., 47 (1951) 591-597.
5 C. Walling and A. Goosen, J. Am. Chem. Soc., 95 (1973) 2987-2991.
6 M.L. Kremer, Trans. Faraday Soc., 59 (1963) 2535-2542.
7 J.T. Groves and M. Van Der Puy, J. Am. Chem. Soc., 98 (1976) 5290-5296.
8 C.F. Wells and D. Mays, J. Chem Soc. A, (1968) 665-668.
9 G. Davies, L.J. Kirschenbaum, and K. Kustin, Inorg. Chem. 7 (1968) 146-154.
10 C.F. Wells and D. Fox, J. Inorg. Nucl. Chem., 38 (1976) 107-112.
11 T.E. Jones and R.E. Hamm, Inorg. Chem., 13 (1974) 1940-1943.
12 E.N. Rizkella, S.S. Anis, and L.H.Khalil, Polyhedron, 6 (1987) 403-409
13 M.E. Bodini, L.A. Willis, T.L. Reichel, and D.T. Sawyer, Inorg. Chem., 15 (1976) 1538-1543.
14 M.E. Bodini and D.T. Sawyer, J. Am. Chem. Soc., 98 (1976) 8366-8371.
15 N.M. Guindy, J.A. Daoud, and N.E. Milad, Egypt. J. Chem., 20 (1977) 131-139.
16 J.L. Deutsch and S.M. Poling, J. Chem. Ed., 46 (1969) 167-168.
17 SAS/STAT User's Guide, version 6, 4th ed., SAS Institute Inc., Cary, North Carolina,1990, pp 1136-1193.
18 B. Carnahan, H.A. Luther, and J.O. Wilkes, Applied Numerical Methods, John Wiley and Sons, New York, 1969, pp 319-329.
19 N. Oishi, Y. Nishida, and S. Kida, Chem. Lett., (1982) 409-410.
20 M. van Duin, J.A. Peters, A.P.G. Kierboom, and H. van Bekkum, J. Chem. Soc. Perkin Trans. II, (1987) 473-480.
21 M. van Duin, J.A. Peters, A.P.G. Kierboom, and H. van Bekkum, J. Chem. Soc. Perkin Trans. II, (1987) 2051-2055.
22 L.J. Boucher and C.G. Coe, Inorg. Chem., 14 (1975) 1289-1295.